catalysts

MDPI

Article

In Situ Regeneration and Deactivation of Co-Zn/H-Beta Catalysts in Catalytic Reduction of NO_x with Propane

Hua Pan [1], Dongmei Xu [1], Chi He [2,*] and Chao Shen [1,*]

[1] College of Biology and Environment Engineering, Zhejiang Shuren University, Hangzhou 310015, China; panhua.7@163.com (H.P.); dm25xu@163.com (D.X.)

[2] School of Energy and Power Engineering, Xi'an Jiaotong University, Xi'an 710049, China

* Correspondence: chi_he@xjtu.edu.cn (C.H.); shenchaozju@hotmail.com (C.S.); Tel.: +86-029-82668572 (C.H.); +86-0571-88297172 (C.S.)

Received: 23 October 2018; Accepted: 24 December 2018; Published: 30 December 2018

Abstract: Regeneration and deactivation behaviors of Co-Zn/H-Beta catalysts were investigated in NO_x reduction with C_3H_8. Co-Zn/H-Beta exhibited a good water resistance in the presence of 10 vol.% H_2O. However, there was a significant drop off in N_2 yield in the presence of SO_2. The formation of surface sulfate and coke decreased the surface area, blocked the pore structure, and reduced the availability of active sites of Co-Zn/H-Beta during the reaction of NO reduction by C_3H_8. The activity of catalyst regenerated by air oxidation followed by H_2 reduction was higher than that of catalyst regenerated by H_2 reduction followed by air oxidation. Among the catalysts regenerated by air oxidation followed by H_2 reduction with different regeneration temperatures, the optimal regeneration temperature was 550 °C. The textural properties of poisoned catalysts could be restored to the levels of fresh catalysts by the optimized regeneration process. The regeneration process of air oxidation followed by H_2 reduction could recover the active sites of cobalt and zinc species from sulfate species, as well as eliminate coke deposition on poisoned catalysts. The regeneration pathway of air oxidation followed by H_2 reduction is summarized as initial removal of coke by air oxidation and final reduction of the sulfate species by H_2.

Keywords: sulfur poisoning; coke deposition; *in situ* regeneration; Co-Zn/H-Beta; NO_x reduction by C_3H_8

1. Introduction

Selective catalytic reduction of NO_x by hydrocarbons (HC-SCR) was considered a promising technology for NO_x removal [1]. Among the HC-SCR catalysts, Co/Beta has attracted much attention due to its excellent activity and N_2 selectivity [2–7]. The long-term stability [3], nature of active sites [4], influences of Co loading and precursor [5], preparation method [6], and mechanism of HC-SCR [7] have been widely investigated on Co/Beta, especially for C_3H_8-SCR [2–6]. To improve the stability and activity of Co/zeolites in HC-SCR, many studies also focused on the modification of Co/zeolites by adding promoters, such as Co-Pd/HBeta [8], Co-In/ferrierite [9], and Co-Zn/HZSM-5 [10].

Sulfur tolerance is a great challenge for deNO_x catalysts. Unfortunately, Co-based zeolites exhibited unsatisfactory activity in the presence of SO_2 [11,12]. On the other hand, coke formation, originating from hydrocarbons, also resulted in the deactivation of deNO_x catalysts for HC-SCR [13]. H_2 reduction is widely used for the regeneration treatment of catalysts deactivated by SO_2, such as NO_x storage-reduction (NSR) catalysts [14–18], and catalytic reduction of NO by NH_3 (NH_3-SCR) catalysts [19,20]. In the case of catalysts deactivated by coke deposition, air calcination was considered as an efficient regeneration method [21–25]. Hence, a regeneration process that combines H_2 reduction

with air oxidation may be a potential technology for *in situ* regeneration of deNO$_x$ catalysts in HC-SCR. To our knowledge, no reports focused on the regeneration of HC-SCR catalysts deactivated by dual impacts of SO_2 and coke deposition.

In the present paper, Co-Zn/H-Beta was chosen as a deNO$_x$ catalyst for C_3H_8-SCR, because it showed good catalytic activity [26]. The regeneration of Co-Zn/H-Beta catalysts deactivated by SO_2 and coke deposition was performed in a combined *in situ* process of air oxidation and H_2 reduction. The effects of the regeneration sequence and regeneration temperature on the regeneration efficiency were investigated.

2. Results and Discussion

2.1. Stability of Catalyst

Figure 1 illustrates the influences of SO_2 and H_2O on the activity of Co-Zn/H-Beta at 450 °C for 80 h. Co-Zn/H-Beta had excellent catalytic activity, with 95% N_2 yield obtained for C_3H_8-SCR at 450 °C without addition of SO_2 and H_2O. The catalytic activity decreased slightly in the presence of 10 vol.% H_2O. Upon removing H_2O from the feeding gas, N_2 yield almost returned to its original level. This demonstrates that Co-Zn/H-Beta displays a good water resistance. However, N_2 yield declined significantly during 50–200 ppm SO_2 co-feeding for 15 h. Only 64% N_2 yield was achieved when 200 ppm SO_2 was added into the feeding gas. Upon switching off the SO_2, N_2 yield increased from 64% to 71.5%, which was far away from the initial activity of 95%. When both 10 vol.% H_2O and 200 ppm SO_2 were added simultaneously for 7 h, N_2 yield further dropped from 71.5% to 62%. Upon switching off the SO_2 and H_2O, a partial recovery of catalytic activity was observed. However, N_2 yield decreased gradually after aging for 40 h without adding SO_2 and H_2O. After the stability experiment, the color of the catalyst turned from light gray to black. This demonstrates that carbon deposition occurs on Co-Zn/H-Beta catalysts during the reaction of NO reduction by C_3H_8.

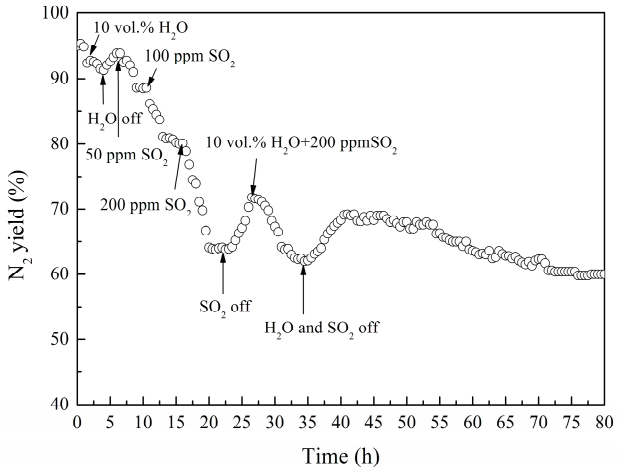

Figure 1. The stability of Co-Zn/H-Beta in C_3H_8-SCR under the dual effects of SO_2 and H_2O.

2.2. Regeneration Performance

Figure 2 presents the influence of regeneration sequence on the activity of the poisoned catalyst at a fixed regeneration temperature of 450 °C. Compared with the poisoned Co-Zn/H-Beta-D catalysts, the regenerated catalysts exhibited higher activity. The activity of regenerated catalysts decreased in the order of: Co-Zn/H-Beta-R (O_2 + H_2, 450 °C) > Co-Zn/H-Beta-R (H_2 + O_2, 450 °C) > Co-Zn/H-Beta-R (H_2, 450 °C) > Co-Zn/H-Beta-R (O_2, 450 °C). Interestingly, Co-Zn/H-Beta-R (O_2 + H_2, 450 °C) displayed higher activity than Co-Zn/H-Beta-R (H_2 + O_2, 450 °C). This suggests that combined regeneration is better than single regeneration, and air oxidation followed by H_2 reduction is an optimal regeneration sequence for the deactivated Co-Zn/H-Beta catalyst in C_3H_8-SCR.

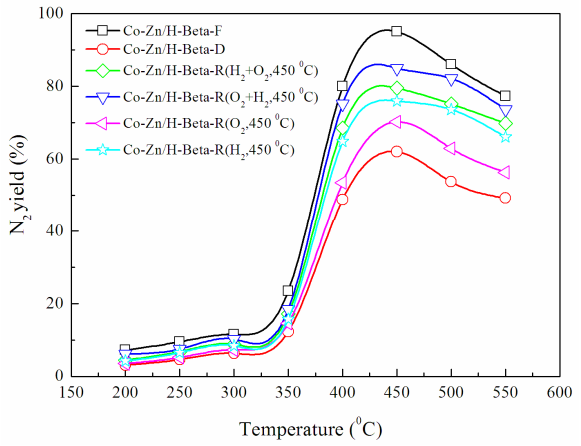

Figure 2. Optimization of regeneration sequence.

Figure 3 exhibits the effect of regeneration temperatures on the activity of the catalysts regenerated by the combined regeneration process. The catalytic activity of both Co-Zn/H-Beta-R (O_2 + H_2) and Co-Zn/H-Beta-R (H_2 + O_2) catalysts increased with the regeneration temperature from 450 to 550 °C. The regenerated Co-Zn/H-Beta-R (O_2 + H_2, 550 °C) displayed similar activity to the fresh catalyst. This indicates that the optimal regeneration temperature was 550 °C. Compared to off-site treatment of solution washing [27] and *in situ* regeneration by H_2 reduction for deactivated deNO$_x$ catalysts [28], the *in situ* regeneration process of air oxidation followed by H_2 reduction showed more convenient operation and higher regeneration efficiency, respectively. Thus, although this comparison may be taken with caution because different reaction conditions were employed, the *in situ* regeneration process of air oxidation followed by H_2 reduction is a promising technology for the regeneration of deactivated Co-Zn/H-Beta catalyst.

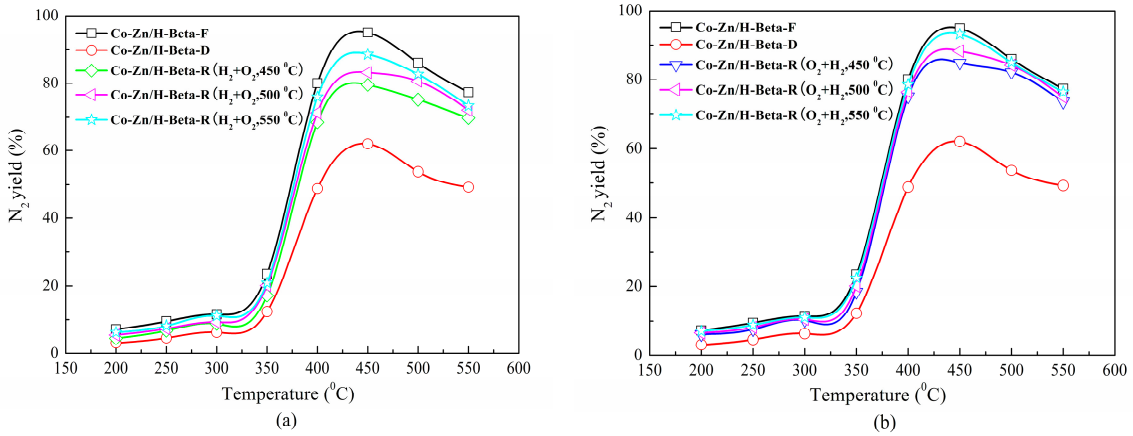

Figure 3. Optimization of regeneration temperature for (**a**) H_2 reduction followed by air oxidation and (**b**) air oxidation followed by H_2 reduction.

2.3. Structural and Textural Properties of Catalysts

Table 1 illustrates the textural properties of the samples. Compared with the Co-Zn/H-Beta-F sample, a significant decrease in surface area, microporous area, and pore volume was detected for the Co-Zn/H-Beta-D catalysts. This implies that sulfate species and coke were deposited both on the surface and in the micropores of the deactivated catalysts. For the regenerated catalysts, surface area, microporous area, and pore volume greatly increased after both the combined regeneration process and single regeneration process. Co-Zn/H-Beta-R (O_2 + H_2, 550 °C) even showed similar values of textural properties to the fresh sample. This implies that air oxidation followed by H_2 reduction at 550 °C could eliminate the sulfates and coke deposited over the deactivated Co-Zn/H-Beta.

Table 1. Textural properties and X-ray photoelectron spectroscopy (XPS) results of samples.

Sample	S_{BET} [a] ($m^2\ g^{-1}$)	S_{micro} [b] ($m^2\ g^{-1}$)	V_{total} [a] ($cm^3\ g^{-1}$)	Binding Energy of $Co2p_{3/2}$ (eV)	Interval between $Co2p_{3/2}$ and $Co2p_{1/2}$ (eV)
Co-Zn/H-Beta-F	428.42	338.88	0.17	780.5	15.8
Co-Zn/H-Beta-D	333.65	264.14	0.13	778.6	17.2
Co-Zn/H-Beta-R (O_2, 550 °C)	384.56	298.22	0.15	/	/
Co-Zn/H-Beta-R (H_2, 550 °C)	360.12	282.36	0.14	/	/
Co-Zn/H-Beta-R (H_2 + O_2, 450 °C)	388.50	305.97	0.15	782.7	14.6
Co-Zn/H-Beta-R (O_2 + H_2, 450 °C)	418.49	323.97	0.16	781.5	15.2
Co-Zn/H-Beta-R (O_2 + H_2, 500 °C)	419.91	336.47	0.17	781.4	15.1
Co-Zn/H-Beta-R (O_2 + H_2, 550 °C)	426.54	337.37	0.17	782.5	15.1

[a] BET method. [b] t-Plot method.

The X-ray diffraction patterns (XRD) of Co-Zn/H-Beta catalysts are shown in Figure 4. The position of the main diffraction peak around 2θ = 22.4° is generally taken as evidence of lattice contraction/expansion of the Beta structure [29,30]. The peaks at 21.8°, 25.1°, 28.4°, 29.3°, and 43.6° were assigned to Beta-type zeolite. The deactivated and regenerated catalysts preserved the typical Beta crystal structure. The diffraction peaks of Co_3O_4 (PDF#73-1701), CoO (PDF#71-1178), and $Zn(OH)_2$ (PDF#74-0094 and PDF#71-2115) were detected for all samples. However, the diffraction peak intensity of $Zn(OH)_2$ in the deactivated catalyst was weaker than in the fresh and regenerated samples. No new peak related to sulfate species was observed on any sample. This implies that sulfate species might exist as amorphous bulk species, which could not be detected by XRD.

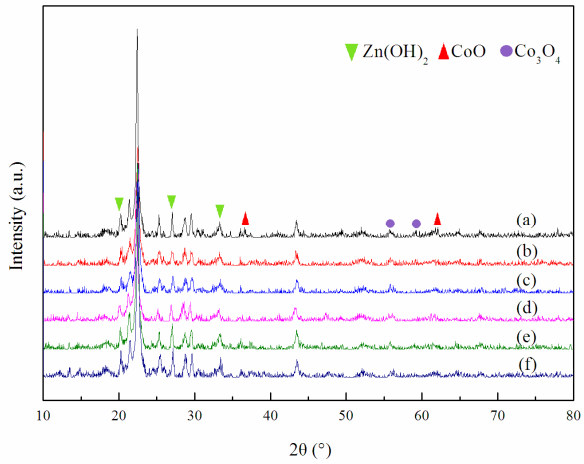

Figure 4. XRD patterns of Co-Zn/H-Beta catalysts. (**a**) Co-Zn/H-Beta-F, (**b**) Co-Zn/H-Beta-D, (**c**) Co-Zn/H-Beta-R (H_2 + O_2, 450 °C), (**d**) Co-Zn/H-Beta-R (O_2 + H_2, 450 °C), (**e**) Co-Zn/H-Beta-R (O_2 + H_2, 500 °C), (**f**) Co-Zn/H-Beta-R (O_2 + H_2, 550 °C).

To identify the state of surface species on various catalysts, the samples were measured by XPS. In Figure 5, the significant movement of the binding energy value of Co $2p_{3/2}$ was observed for both deactivated and regenerated samples, compared to the fresh sample. The binding energy of Co $2p_{3/2}$ shifted toward a lower value (778.6 eV) in the deactivated catalyst. However, the Co $2p_{3/2}$ peaks of regenerated catalysts were shifted to a higher binding energy (781.4–782.7 eV). In Co 2p spectra, shake-up peaks were observed for all samples. This means that metallic cobalt was absent in all samples, because the spectrum of metallic cobalt does not contain shake-up satellite structure at all [31]. Table 1 illustrates the results of Co 2p in the fresh, deactivated, and regenerated catalysts. According to the position of the Co $2p_{3/2}$ peak and interval between Co $2p_{3/2}$ and Co $2p_{1/2}$, CoO, Co_3O_4, $Co(OH)_2$, and $ZnCo_2O_4$ were present in the fresh sample [32,33]. For the deactivated catalyst, the lowest binding energy of Co $2p_{3/2}$ (778.6 eV) and highest interval between Co $2p_{3/2}$ and Co $2p_{1/2}$ (17.2 eV) were observed, which was quite different from other catalysts in Table 1. This implies that sulfate species were generated on the surface of the deactivated catalyst. For Co-Zn/H-Beta-R

(H_2 + O_2, 450 °C), the highest binding energy of Co $2p_{3/2}$ (782.7 eV) and lowest interval between Co $2p_{3/2}$ and Co $2p_{1/2}$ (14.6 eV) were detected among all catalysts. Cobalt species mainly exist as a $CoAl_2O_4$ state on Co-Zn/H-Beta-R (H_2 + O_2, 450 °C) [33]. $CoAl_2O_4$ was recognized to be inactive for NO-SCR [34,35]. Thus, the catalytic activity of Co-Zn/H-Beta-R (H_2 + O_2, 450 °C) was lower than that of Co-Zn/H-Beta-R (O_2 + H_2) catalysts (Figure 2). In the case of Co-Zn/H-Beta-R (O_2 + H_2) catalysts, the binding energy value of Co $2p_{3/2}$ was from 781.4 to 782.5 eV, and the interval between Co $2p_{3/2}$ and Co $2p_{1/2}$ was about 15.1 eV. This indicates that CoO, Co_3O_4, $Co(OH)_2$, and $ZnCo_2O_4$ were present in Co-Zn/H-Beta-R (O_2 + H_2) catalysts [32,33]. Therefore, the regeneration process of air oxidation followed by H_2 reduction could promote the recovery of the deactivated cobalt species.

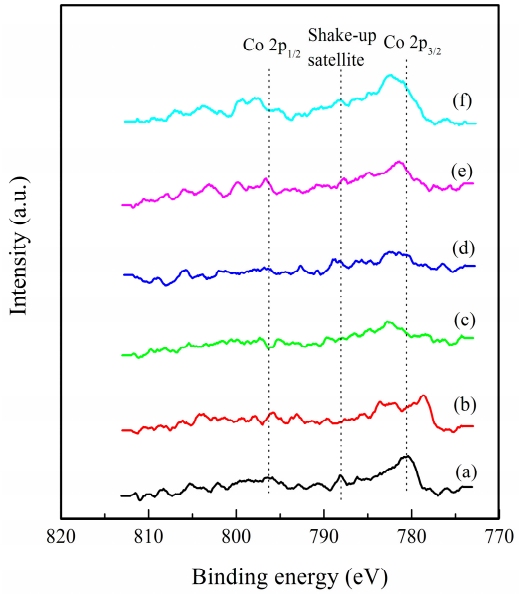

Figure 5. XPS spectra of the Co 2p regions for fresh, deactivated, and regenerated catalysts. (**a**) Co-Zn/H-Beta-F, (**b**) Co-Zn/H-Beta-D, (**c**) Co-Zn/H-Beta-R (H_2 + O_2, 450 °C), (**d**) Co-Zn/H-Beta-R (O_2 + H_2, 450 °C), (**e**) Co-Zn/H-Beta-R (O_2 + H_2, 500 °C), (**f**) Co-Zn/H-Beta-R (O_2 + H_2, 550 °C).

Figure 6 presents XPS spectra of the Zn 2p regions for the fresh, deactivated, and regenerated catalysts. For all samples, binding energy of Zn $2p_{3/2}$ and interval between Zn $2p_{3/2}$ and Zn $2p_{1/2}$ were 1022–1023 eV and 23 eV, respectively, which could be attributed to $Zn(OH)^+$ [36] or ZnO [37]. Compared to the fresh sample, a lower binding energy of Zn $2p_{3/2}$ was observed for the deactivated sample, which was similar with the variation trend of Co $2p_{3/2}$ lines. The binding energy of Zn $2p_{3/2}$ shifting to a lower value may be due to the formation of sulfate species on the surface of the deactivated catalysts. For Co-Zn/H-Beta-R (O_2 + H_2) catalysts, the position of the binding energy of Zn $2p_{3/2}$ and Zn $2p_{1/2}$ was the same as the fresh sample. However, a lower binding energy of Zn $2p_{3/2}$ and Zn $2p_{1/2}$ was also observed for Co-Zn/H-Beta-R (H_2 + O_2, 450 °C), which was similar with the deactivated sample. Thus, regeneration sequence was important to the regeneration of poisoned catalysts. The peak intensity of both Co $2p_{3/2}$ and Zn $2p_{3/2}$ was enhanced with the increase of regeneration temperature from 450 to 550 °C, meaning that a regeneration temperature of 550 °C is optimal.

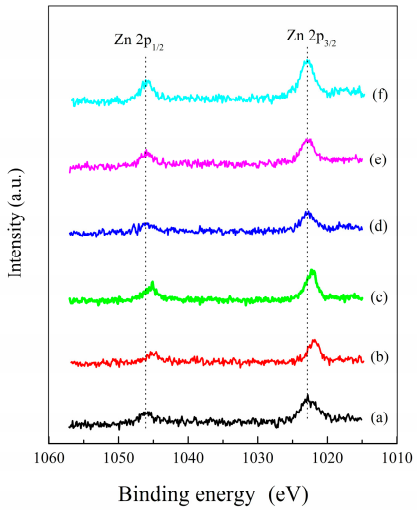

Figure 6. XPS spectra of the Zn 2p regions for fresh, deactivated, and regenerated catalysts. (**a**) Co-Zn/H-Beta-F, (**b**) Co-Zn/H-Beta-D, (**c**) Co-Zn/H-Beta-R (H_2 + O_2, 450 °C), (**d**) Co-Zn/H-Beta-R (O_2 + H_2, 450 °C), (**e**) Co-Zn/H-Beta-R (O_2 + H_2, 500 °C), (**f**) Co-Zn/H-Beta-R (O_2 + H_2, 550 °C).

Figure 7 presents the H_2-temperature programmed reduction (H_2-TPR) of Co-Zn/H-Beta catalysts. The TPR peak centered at around 345 °C is ascribed to the reduction of Co_3O_4 [38]. The peaks centered at 423 °C and 512 °C could correspond to the reduction of CoO_x on the catalyst surface and in the catalyst pore, respectively [38]. The broad peaks centered at 550 °C and 565 °C could be ascribed to the reduction of sulfate and $CoAl_2O_4$, respectively. The high temperature reduction peaks of 620 °C and 800 °C may be assigned to the reduction peaks of $Zn(OH)^+$ and ZnO, respectively. The reduction peak of sulfate (550 °C) is clearly detected for Co-Zn/H-Beta-D and Co-Zn/H-Beta-R (O_2, 450 °C) catalysts. Thus, air oxidation could not remove sulfate on deactivated catalysts. The reduction peak of $CoAl_2O_4$ was observed for Co-Zn/H-Beta-R (H_2 + O_2, 450 °C), but not for Co-Zn/H-Beta-R (O_2 + H_2, 450 °C), Co-Zn/H-Beta-R (O_2 + H_2, 550 °C), and Co-Zn/H-Beta-R (H_2, 450 °C). This may be due to the diffusion of Co species on the surface into the pore of zeolite, and interaction with extra-framework Al^{3+} cations at high temperature during the SCR reaction and regeneration process, resulting in the formation of $CoAl_2O_4$ [39]. This means that air oxidation can promote the formation of $CoAl_2O_4$, while H_2 reduction could inhibit $CoAl_2O_4$ formation. $CoAl_2O_4$ was recognized to be inactive for HC-SCR [34,35]. Therefore, air oxidation followed by H_2 reduction is an optimal regeneration sequence for the deactivated Co-Zn/H-Beta catalysts in C_3H_8-SCR.

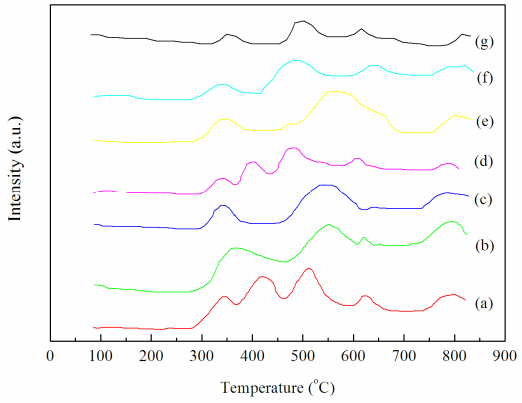

Figure 7. H_2-TPR of fresh, deactivated, and regenerated catalysts. (**a**) Co-Zn/H-Beta-F, (**b**) Co-Zn/H-Beta-D, (**c**) Co-Zn/H-Beta-R (O_2, 550 °C), (**d**) Co-Zn/H-Beta-R (H_2, 550 °C), (**e**) Co-Zn/H-Beta-R (H_2 + O_2, 450 °C), (**f**) Co-Zn/H-Beta-R (O_2 + H_2, 450 °C), (**g**) Co-Zn/H-Beta-R (O_2 + H_2, 550 °C).

Figure 8 shows thermo gravimetric analysis (TGA) curves of various catalysts. The weight loss of all samples in the temperature range of 50–200 °C can be attributed to the desorption of H_2O. However, the deactivated catalyst displayed another stage of weight losses at temperatures above 650 °C, which corresponded to the combustion of coke and sulfate deposited on the catalyst. The regenerated (Co-Zn/H-Beta-R (H_2 + O_2, 450 °C)) sample showed slighter weight losses than the deactivated sample did at temperatures above 650 °C. Interestingly, no significant weight losses were observed for the regenerated (Co-Zn/H-Beta-R (O_2 + H_2, 550 °C)) sample. This further indicates that a combined *in situ* regeneration process of air oxidation followed by H_2 reduction at 550 °C is efficient for regeneration of Co-Zn/H-Beta in C_3H_8-SCR. In summary, the regeneration pathway is illustrated in Scheme 1. Coke on the deactivated catalyst was initially removed by air oxidation at 550 °C. Finally, the sulfate species were reduced to the active cobalt and zinc species by H_2 at 550 °C.

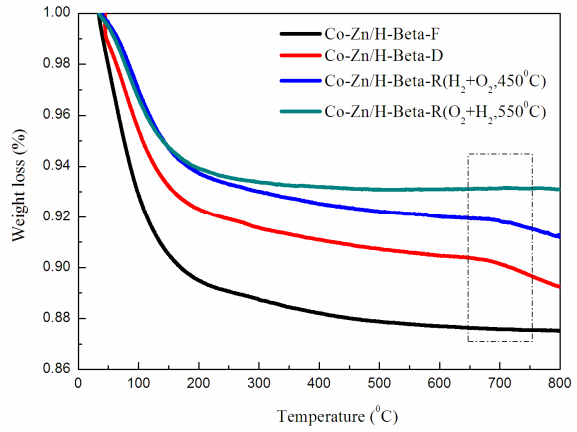

Figure 8. TGA curves of fresh, deactivated, and regenerated catalysts.

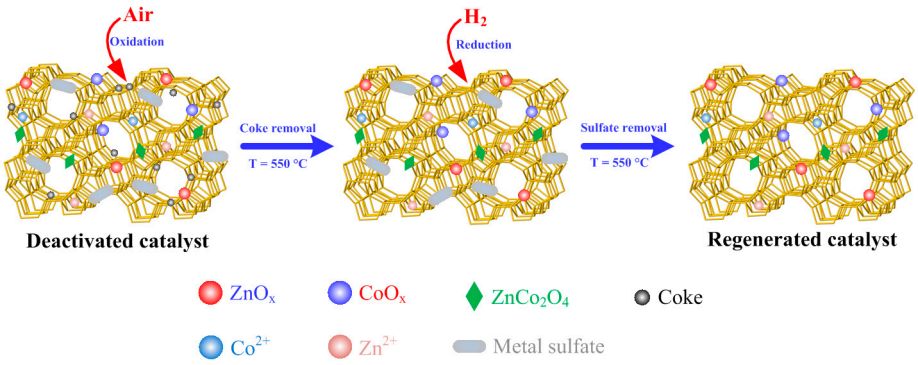

Scheme 1. Regeneration pathway for the combined polluted Co-Zn/H-Beta catalyst.

3. Materials and Methods

3.1. Catalyst Preparation

Beta zeolite with an atomic ratio Si/Al = 25 was purchased commercially in H-form from Nankai University (Tianjin, China). Co-Zn/H-Beta catalysts were synthesized according to the method described elsewhere [40], using $Co(NO_3)_2$ and $Zn(NO_3)_2$ as precursors. All the chemicals were purchased from Macklin Inc. (Shanghai, China). The cobalt and zinc content of Co-Zn/H-Beta was 2 wt.%. The fresh samples were noted as Co-Zn/H-Beta-F.

3.2. Deactivation and Regeneration of Catalysts

In the deactivation process, the samples were exposed to a mixture of 50–200 ppm SO_2, 600 ppm NO, 25 ppm NO_2, 600 ppm C_3H_8, 6 vol.% O_2, 10 vol.% H_2O, and balance of N_2 at 450 °C for 45 h.

The deactivated catalysts were denoted as Co-Zn/H-Beta-D. All the gases were purchased from Hangzhou Jingong Special Gas Co., Ltd. (Hangzhou, China).

The deactivated catalysts were regenerated by 60 mL min^{-1} air and 400 mL min^{-1} 5 vol.% H_2/Ar at regeneration temperatures from 450 to 550 °C for 60 min. The regenerated catalysts were denoted as Co-Zn/H-Beta-R (O_2, H_2, O_2 + H_2, and H_2 + O_2, T), where O_2 means that the deactivated catalysts were regenerated by air oxidation, and H_2 means that the deactivated catalysts were regenerated by H_2 reduction. O_2 + H_2 means that the deactivated catalysts were regenerated by air oxidation followed by H_2 reduction. H_2 + O_2 means that the deactivated catalysts were regenerated by H_2 reduction followed by air oxidation. T is the regeneration temperature.

3.3. Catalytic Activity Measurement

Catalytic activity tests were performed in a self-made packed-bed flow micro-reactor (1 cm i.d.), operating at atmospheric pressure. A 1.5 mL (0.73 g) volume of catalyst powder was held on a quartz frit at the center of the reactor. A typical feeding gas composition was 600 ppm NO, 25 ppm NO_2, 600 ppm C_3H_8, and 6 vol.% O_2, with N_2 as the balance gas. Each feeding gas flow rate was controlled independently by a mass flow controller (D07, Beijing Sevenstar Electronics Co.,Ltd., Beijing, China). The overall flow rate was 460 mL min^{-1}, which was equal to a space velocity of 18,400 h^{-1}.

NO and NO_2 concentrations were continuously monitored by an infrared gas analyzer (Xi'an Juneng Corporation, Xi'an, China). The products were analyzed using a gas chromatograph (Linghua GC9890, Shanghai Ling-Hua Instrument Co., Ltd, Shanghai, China) equipped with a thermal conductivity detector (TCD). A porapak Q column (Shanghai Ling-Hua Instrument Co., Ltd., Shanghai, China) was used for separation of CO_2, N_2O and NO. The data was collected in the steady state reaction. In this work, N_2 selectivity is over 95%, because N_2O concentration is below 10 ppm. Thus, the catalytic activity was assessed in terms of the following equation:

$$N_2 \text{ yield } (\%) = \frac{(NO_{in} + NO_{2,in}) - (NO_{out} + NO_{2,out} + 2N_2O_{out})}{(NO_{in} + NO_{2,in})} \times 100\% \quad (1)$$

3.4. Catalyst Characterizations

N_2 adsorption isotherms (ASAP2460, Micromeritics Instrument (Shanghai) Ltd., Shanghai, China) and XRD (Rigaku, Tokyo, Japan) and XPS (PHI-5000C ESCA system, Perkin–Elmer, Waltham, MA, USA) measurements were carried out according to the method described in our previous work [41]. TGA was conducted on an HCR-3 analyzer (Beijing Henven Scientific Instrument Co., Ltd., Beijing, China) from 30 to 800 °C under air, with a heating rate of 5 °C/min.

4. Conclusions

Co-Zn/H-Beta catalysts exhibited a poor stability in the presence of SO_2 and H_2O for C_3H_8-SCR, due to SO_2 poisoning and carbon deposition. The formation of surface sulfate and coke reduced the availability of surface active sites and textural properties of the catalysts. Coke deposition and surface sulfate could be reduced by the combined processes of air oxidation followed by H_2 reduction *in situ*. The combined process of air oxidation followed by H_2 reduction is an available technology for the regeneration of Co-Zn/H-Beta catalysts in C_3H_8-SCR, for removing NO_x from lean-burn and diesel exhausts.

Author Contributions: Conceptualization, H.P. and C.H.; Investigation, H.P. and D.X.; Supervision, C.S.; Writing-original draft, H.P.

Funding: This work was financially supported by the National Natural Science Foundation of China (21677114), Natural Science Foundation of Zhejiang Province of China (LY19E080023), and Young and middle-aged academic team project of Zhejiang Shuren University. We also acknowledge the support of Key Laboratory of Microbial Technology for Industrial Pollution Control of Zhejiang Province.

Conflicts of Interest: The authors declare no conflict of interest.

References

1. Mendes, A.N.; Ribeiro, M.F.; Henriques, C.; Da Costa, P. On the Effect of Preparation Methods of PdCe-MOR Catalysts as NO_x CH_4-SCR System for Natural Gas Vehicles Application. *Catalysts* **2015**, *5*, 1815–1830. [CrossRef]
2. Tabata, T.; Ohtsuka, H.; Sabatino, L.M.F.; Bellussi, G. Selective catalytic reduction of NO_x by propane on Co-loaded zeolites. *Microporous Mesoporous Mater.* **1998**, *21*, 517–524. [CrossRef]
3. Tabata, T.; Kokitsu, M.; Ohtsuka, H.; Okada, O.; Sabatino, L.M.F.; Bellussi, G. Study on catalysts of selective reduction of NO_x using hydrocarbons for natural gas engines. *Catal. Today* **1996**, *27*, 91–98. [CrossRef]
4. Ohtsuka, H.; Tabata, T.; Okada, O.; Sabatino, L.M.F.; Bellussi, G. A study on selective reduction of NO_x by propane on Co-Beta. *Catal. Lett.* **1997**, *44*, 265–270. [CrossRef]
5. Chen, H.H.; Shen, S.C.; Chen, X.Y.; Kawi, S. Selective catalytic reduction of NO over Co/beta-zeolite: Effects of synthesis condition of beta-zeolites, Co precursor, Co loading method and reductant. *Appl. Catal. B Environ.* **2004**, *50*, 37–47. [CrossRef]
6. Čapek, L.; Dědeček, J.; Sazama, P.; Wichterlová, B. The decisive role of the distribution of Al in the framework of beta zeolites on the structure and activity of Co ion species in propane-SCR–NO_x in the presence of water vapour. *J. Catal.* **2010**, *272*, 44–54. [CrossRef]
7. Pietrzyk, P.; Dujardin, C.; Gora-Marek, K.; Granger, P.; Sojka, Z. Spectroscopic IR, EPR, and operando DRIFT insights into surface reaction pathways of selective reduction of NO by propene over the Co–BEA zeolite. *Phys. Chem. Chem. Phys.* **2012**, *14*, 2203–2215. [CrossRef]
8. Ferreira, A.P.; Henriques, C.; Ribeiro, M.F.; Ribeiro, F.R. SCR of NO with methane over Co-HBEA and PdCo-HBEA catalysts: The promoting effect of steaming over bimetallic catalyst. *Catal. Today* **2005**, *107–108*, 181–191. [CrossRef]
9. Kubacka, A.; Janas, J.; Sulikowski, B. In/Co-ferrierite: A highly active catalyst for the CH_4-SCR NO process under presence of steam. *Appl. Catal. B Environ.* **2006**, *69*, 43–48. [CrossRef]
10. Ren, L.L.; Zhang, T.; Liang, D.B.; Xu, C.H.; Tang, J.W.; Lin, L.W. Effect of addition of Zn on the catalytic activity of a Co/HZSM-5 catalyst for the SCR of NO_x with CH_4. *Appl. Catal. B Environ.* **2002**, *35*, 317–321. [CrossRef]
11. Zhang, J.Q.; Liu, Y.Y.; Fan, W.B.; He, Y.; Li, R.F. Effect of SO_2 on Catalytic Performance of CoH-FBZ for Selective Catalytic Reduction of NO by CH_4 in The Presence of O_2. *Environ. Eng. Sci.* **2007**, *24*, 292–300. [CrossRef]
12. Chen, S.W.; Yan, X.L.; Wang, Y.; Chen, J.Q.; Pan, D.H.; Ma, J.H.; Li, R.F. Effect of SO_2 on Co sites for NO-SCR by CH_4 over Co-Beta. *Catal. Today* **2011**, *175*, 12–17. [CrossRef]
13. Krishna, K.; Makkee, M. Coke formation over zeolites and CeO_2-zeolites and its influence on selective catalytic reduction of NO_x. *Appl. Catal. B Environ.* **2005**, *59*, 35–44. [CrossRef]
14. Corbos, E.C.; Courtois, X.; Bion, N.; Marecot, P.; Duprez, D. Impact of the support oxide and Ba loading on the sulfur resistance and regeneration of Pt/Ba/support catalysts. *Appl. Catal. B Environ.* **2008**, *80*, 62–71. [CrossRef]
15. Wang, Q.; Zhu, J.H.; Wei, S.Y.; Chung, J.S.; Guo, Z.H. Sulfur Poisoning and Regeneration of NO_x Storage-Reduction $Cu/K_2Ti_2O_5$ Catalyst. *Ind. Eng. Chem. Res.* **2010**, *49*, 7330–7335. [CrossRef]
16. Liu, Z.Q.; Anderson, J.A. Influence of reductant on the regeneration of SO_2-poisoned $Pt/Ba/Al_2O_3$ NO_x storage and reduction catalyst. *J. Catal.* **2004**, *228*, 243–253. [CrossRef]
17. Tanaka, T.; Amano, K.; Dohmae, K.; Takahashi, N.; Shinjoh, H. Studies on the regeneration of sulfur-poisoned NO_x storage and reduction catalysts, including a Ba composite oxide. *Appl. Catal. A Gen.* **2013**, *455*, 16–24. [CrossRef]
18. Le Phuc, N.; Corbos, E.C.; Courtois, X.; Can, F.; Marecot, P.; Duprez, D. NO_x storage and reduction properties of $Pt/Ce_xZr_{1-x}O_2$ mixed oxides: Sulfur resistance and regeneration, and ammonia formation. *Appl. Catal. B Environ.* **2009**, *93*, 12–21. [CrossRef]
19. Doronkin, D.E.; Khan, T.S.; Bligaard, T.; Fogel, S.; Gabrielsson, P.; Dahl, S. Sulfur poisoning and regeneration of the Ag/γ-Al_2O_3 catalyst for H_2-assisted SCR of NO_x by ammonia. *Appl. Catal. B Environ.* **2012**, *117*, 49–58. [CrossRef]
20. Chang, H.Z.; Li, J.H.; Yuan, J.; Chen, L.; Dai, Y.; Arandiyan, H.; Xu, J.Y.; Hao, J.M. Ge, Mn-doped CeO_2–WO_3 catalysts for NH_3–SCR of NO_x: Effects of SO_2 and H_2 regeneration. *Catal. Today* **2013**, *201*, 139–144. [CrossRef]

21. Serrano, D.P.; Aguado, J.; Rodríguez, J.M.; Peral, A. Catalytic cracking of polyethylene over nanocrystalline HZSM-5: Catalyst deactivation and regeneration study. *J. Anal. Appl. Pyrol.* **2007**, *79*, 456–464. [CrossRef]
22. Aguado, J.; Serrano, D.P.; Escola, J.M.; Briones, L. Deactivation and regeneration of a Ni supported hierarchical Beta zeolite catalyst used in the hydroreforming of the oil produced by LDPE thermal cracking. *Fuel* **2013**, *109*, 679–686. [CrossRef]
23. Madaan, N.; Gatla, S.; Kalevaru, V.N.; Radnik, J.; Lücke, B.; Brückner, A.; Martin, A. Deactivation and regeneration studies of a $PdSb/TiO_2$ catalyst used in the gas-phase acetoxylation of toluene. *J. Catal.* **2011**, *282*, 103–111. [CrossRef]
24. Villegas, J.I.; Kumar, N.; Heikkilä, T.; Lehto, V.P.; Salmi, T.; Murzin, D.Y. Isomerization of n-butane to isobutane over Pt-modified Beta and ZSM-5 zeolite catalysts: Catalyst deactivation and regeneration. *Chem. Eng. J.* **2006**, *120*, 83–89. [CrossRef]
25. Mazzieri, V.A.; Pieck, C.L.; Vera, C.R.; Yori, J.C.; Grau, J.M. Analysis of coke deposition and study of the variables of regeneration and rejuvenation of naphtha reforming trimetallic catalysts. *Catal. Today* **2018**, *133–135*, 870–878. [CrossRef]
26. Zhang, Y.T.; Pan, H.; Li, W.; Shi, Y. SCR of NO_x with C_3H_8 over Co/H-beta Modified by Zn at High GHSV. *J. Chem. Eng. Chin. Univ.* **2009**, *23*, 236–239.
27. Khodayari, R. Regeneration of commercial TiO_2-V_2O_5-WO_3 SCR catalysts used in bio fuel plants. *Appl. Catal. B Environ.* **2001**, *30*, 87–99. [CrossRef]
28. Pan, H.; Jian, Y.F.; Yu, Y.K.; He, C.; Shen, Z.X.; Liu, H.X. Regeneration and sulfur poisoning behavior of In/H-BEA catalyst for NO_x reduction by CH_4. *Appl. Surf. Sci.* **2017**, *401*, 120–126. [CrossRef]
29. Dzwigaj, S.; Janas, J.; Machej, T.; Che, M. Selective catalytic reduction of NO by alcohols on Co- and Fe-Siβ catalysts. *Catal. Today* **2007**, *119*, 133–136. [CrossRef]
30. Reddy, J.S.; Sayari, A. A simple method for the preparation of active Ti beta zeolite catalysts. *Stud. Surf. Sci. Catal.* **1995**, *94*, 309–316.
31. Chung, K.S.; Massoth, F.E. Studies on molybdena-alumina catalysts: VII. Effect of cobalt on catalyst states and reducibility. *J. Catal.* **1980**, *64*, 320–331. [CrossRef]
32. Stranick, M.S.; Houalla, M.; Hercules, D.M. Spectroscopic characterization of $TiO_2Al_2O_3$ and $CoAl_2O_3TiO_2$ catalysts. *J. Catal.* **1987**, *106*, 362–368. [CrossRef]
33. Zsoldos, Z.; Guczi, L. Structure and Catalytic Activity of Alumina Supported Platinum Cobalt Bimetallic Catalysts. 3. Effect of Treatment on the Interface Layer. *J. Phys. Chem.* **1992**, *96*, 9393–9400. [CrossRef]
34. Gomez-Garcia, M.A.; Pitchon, V.; Kiennemann, A. Pollution by nitrogen oxides: An approach to NO_x abatement by using sorbing catalytic materials. *Environ. Int.* **2005**, *31*, 445–467. [CrossRef] [PubMed]
35. Yan, J.; Kung, M.C.; Sachtler, W.M.H.; Kung, H.H. Co/Al_2O_3 Lean NO_x Reduction Catalyst. *J. Catal.* **1997**, *172*, 178–186. [CrossRef]
36. Gong, T.; Qin, L.J.; Lu, J.; Feng, H. ZnO modified ZSM-5 and Y zeolites fabricated by atomic layer deposition for propane conversion. *Phys. Chem. Chem. Phys.* **2016**, *18*, 601–614. [CrossRef] [PubMed]
37. Kicir, N.; Tuken, T.; Erken, O.; Gumus, C.; Ufuktepe, Y. Nanostructured ZnO films in forms of rod, plate and flower: Electrodeposition mechanisms and characterization. *Appl. Surf. Sci.* **2016**, *377*, 191–199. [CrossRef]
38. Wang, X.; Chen, H.Y.; Sachtler, W.M.H. Catalytic reduction of NO_x by hydrocarbons over Co/ZSM-5 catalysts prepared with different methods. *Appl. Catal. B Environ.* **2000**, *26*, L227–L239. [CrossRef]
39. Zhang, Q.; Wang, X.D. Charaterization of the phase and valency state of Co on Co/HZSM-5 catalysts. *Chem. J. Chin. Univ.* **2002**, *23*, 129–131.
40. Shi, Y.; Su, Q.F.; Chen, J.; Wei, J.W.; Yang, J.T.; Pan, H. Combination non-thermal plasma and low temperature-C_3H_8-SCR over Co-In/H-beta catalyst for NO_x abatement. *Environ. Eng. Sci.* **2009**, *26*, 1107–1113. [CrossRef]
41. Pan, H.; Guo, Y.H.; Bi, H.T. NO_x adsorption and reduction with C_3H_6 over Fe/zeolite catalysts: Effect of catalyst support. *Chem. Eng. J.* **2015**, *280*, 66–73. [CrossRef]